Biochemical Pharmacology, Vol. 28, pp. 1553–1559.

0006-2952/79/0501-1553 $02.00/0

CANNABIDIOL AND Δ^9-TETRAHYDROCANNABINOL METABOLISM

IN VITRO COMPARISON OF MOUSE AND RAT LIVER CRUDE MICROSOME PREPARATIONS

HENRY K. BORYS and RALPH KARLER

Department of Pharmacology, University of Utah College of Medicine, Salt Lake City, UT 84132, U.S.A.

(*Received* 18 *May* 1978; *accepted* 16 *October* 1978)

Abstract—The *in vitro* biotransformations of cannabidiol (CBD) and Δ^9-tetrahydrocannabinol (Δ-THC) by hepatic microsomal preparations from mouse and rat were compared and it was found that both cannabinoids are metabolized approximately two to three times faster by a mouse preparation than by a similar preparation from the rat. In both species, however, CBD was metabolized more slowly than Δ^9-THC. The metabolite patterns resulting from the biotransformations of radioactive CBD and Δ^9-THC were examined by thin-layer chromatography and were found to be qualitatively identical in both the mouse and rat. In contrast, studies of the rate of cannabinoid metabolism in the presence of excess substrate revealed that CBD metabolism was only linear for about 10 min, whereas Δ^9-THC metabolism was linear for about 60 min. This difference was noted in both species. The evidence suggests that CBD metabolism is inhibited by its own metabolites. Furthermore, the results of other experiments indicate that CBD metabolites can also inhibit Δ^9-THC and aminopyrine metabolism. The established ability of CBD to inhibit hepatic microsomal drug metabolism *in vivo* may also be the consequence of the formation of inhibitory metabolites.

Cannabidiol (CBD) is one of the major cannabinoid components of marihuana extract and is known to elicit a number of pharmacological effects. For example, the drug exhibits marked neuropharmacological activity both *in vivo* and *in vitro*, as illustrated by the well-documented anticonvulsant effects of CBD [1, 2] and the ability of CBD to depress post-tetanic potentiation in isolated sympathetic ganglia [3]. Moreover, CBD can inhibit the hepatic mixed-function oxidase system responsible for the biotransformation of drugs [4—8].

The role, if any, which the metabolites of CBD play in its pharmacology is not known, but some of the metabolites of Δ^9-tetrahydrocannabinol (Δ^9-THC) are markedly active and probably contribute to, or may even account for, the properties of the parent compound [9–11]. Many of these metabolites have been identified and synthesized, so that a study of their properties vis-à-vis those of Δ^9-THC has been made feasible. In contrast, less is known about the pharmacological characteristics of CBD metabolites. Aside from this difference, however, the studies of the metabolites of both these cannabinoids have primarily emphasized qualitative measurements. Little attention has been directed toward establishing the pharmacological significance of the metabolites. For example, what is the relationship between the metabolites and the pharmacological activity [12–16]?

The purpose of the present work was to initiate a qualitative and quantitative study of the metabolism of CBD in order to assess the relative significance of CBD and its metabolites in producing a specific pharmacological effect: to wit, the inhibition of the mixed-function oxidase system. One approach to such a study is to use isolated hepatic microsomes. Accordingly, crude microsomal preparations from both the mouse and rat were used in the following investigations of CBD and Δ^9-THC metabolism; the metabolism of the latter compound has been the subject of many reports [12] and therefore, served as a good reference compound to which the metabolism of CBD could be related. Three types of studies were conducted. First, the apparent Michaelis–Menten constants and other kinetic characteristics of CBD and Δ^9-THC metabolism were determined. Secondly, the general patterns of CBD and Δ^9-THC metabolites produced under kinetically similar *in vitro* conditions were compared. Finally, the inhibitory effect of CBD on mixed-function oxidations was investigated, particularly as the inhibition related to the metabolism of CBD.

MATERIALS AND METHODS

Chemicals. Δ^9-THC, 11-hydroxy-Δ^9-THC, 8α,-11,dihydroxy-Δ^9-THC and CBD, and [^{3}H]-Δ^9-THC (101 μCi/mg) and [^{3}H]-CBD (86 μCi/mg) were acquired from the Biomedical Research Branch, Division of Research of the National Institute on Drug Abuse; dimethylamine[^{14}C]aminopyrine (52.8 μCi/mg) was obtained from the Amersham/Searle Corp., Arlington Heights, IL; glucose-6-phosphate, glucose-6-phosphate, glucose-6-phosphate dehydrogenase (GPDH), NADP and nicotinamide were purchased from Sigma Chemicals, St. Louis, MO; the propylene oxide polymer Pluronic F68 and Fast Blue B were supplied by BASF Wyandotte Corp., Wyandotte, MI and Matheson, Coleman & Bell, Norwood, OH respectively. Analytical reagent grade solvents were employed without additional purification. The silica gel thin-layer chromatography (t.l.c.) sheets used to separate the cannabinoids were Eastman type 6061.

Tissue preparation. Male Sprague–Dawley rats weighing 95–100 g and 4 to 5-week-old male Charles River mice (ICR) were used in all the experiments described in the following sections. The livers were removed from rats anesthitized with ether or from mice killed by cervical dislocation; each liver was immediately rinsed in an ice-cold 1.15% KCl solution and subsequently

diced into small fragments which were washed with several volumes of the ice-cold 1.15% KCl. A tissue mash was prepared from the washed fragments by using a small, plastic, sieve-like press and the mash was then homogenized in 4 vol. of 1.15% KCl with a Potter–Elvehjem type tissue grinder consisting of a smooth-glass mortar and Teflon pestle. The homogenate was centrifuged for 20 min at 15,000 rev/min (20,000 *g* at r_{max}) with a Beckman L-2 centrifuge in a Ti-50 rotor. The protein content of the supernatant fraction was determined by the method of Lowry *et al.* [17] with bovine serum albumin as a standard and was found to average 16 mg/ml.

Assays. The solution in which the crude microsomal preparation (20,000 *g* supernatant fraction) was routinely incubated had the following composition (final concentrations): glucose-6-phosphate (10 mM), GPDH (0.5 units/ml), NADP (1 mM), $MgCl_2$ (8 mM), nicotinamide (4 mM) and sodium phosphate buffer (50–100 mM, pH 7.2). Aminopyrine *N*-demethylase activity was determined by the radioisotopic assay of Poland and Nebert [18]. For the measurement of Δ^9-THC and CBD hydroxylase activity, the following procedure was used: Stock suspensions of CBD or Δ^9-THC were prepared prior to each experiment by mixing an aliquot of a 2 per cent solution of the cannabinoid in 95% ethanol with an equal volume of Pluronic F68 (10 mg/ml in 95% ethanol) followed by the stepwise addition of water or a buffer solution to the desired volume. An aliquot of the stock cannabinoid suspension was then added to the incubation medium. Incubation volumes varied from 50 to 250 μl, and the reactions were run in 10 mm o.d. × 75 mm glass culture tubes or 7 mm o.d. × 65 mm glass microtubes.

Although the cannabinoids can be suspended in Pluronic by sonification alone, this approach was not used in the present investigation for two reasons. First, the sonification of very small volumes frequently results in the emission of a fine spray of radioactive cannabinoid, which contaminates the laboratory. Secondly, suspensions of cannabinoids, especially the relatively high concentrations required in the K_m and V_{max} studies, in Pluronic alone are not uniform because some material (detergent–cannabinoid) frequently adheres to the walls of the container. The use of ethanol with Pluronic, however, obviated these suspension problems.

In a separate series of experiments, the effect of various combinations of these two agents on Δ^9-THC metabolism was investigated. In the presence of a fixed amount of ethanol (0.05%), Pluronic in the concentration range of 0.0008 to 0.16% had no effect on the metabolism. Similarly, in the presence of 0.0005% Pluronic, varying concentrations of ethanol up to 0.3% produced only a negligible effect. An ethanol concentration of 0.5%, however, did cause about a 15 per cent depression in Δ^9-THC metabolism. For the K_m and V_{max} determinations, the ethanol concentration was 0.5% and the Pluronic concentration was 0.003%. In all remaining studies, the ethanol concentration never exceeded 0.3% and the Pluronic concentrations never exceeded 0.001%.

After incubation of the 20,000 *g* supernatant fraction at 37°, the samples were transferred to an ice bath, mixed with and equal volume of methanol and centrifuged at room temperature for 10 min at approximately 1000 *g*. The somewhat turbid supernatant fractions were put into clean tubes and a volume of methanol equal to one-half the original incubation volume was added to the pellets. After resuspension of the pellets and centrifugation, the resultant clear supernatant fractions were combined with the first supernatant fractions, and a volume of chloroform equal to the initial volume of the incubation mixture was added. The samples were mixed, centrifuged to separate the phases, and as much of the chloroform layer as possible was pipetted from beneath the aqueous layer and transferred to another set of tubes. The aqueous layer was extracted a second time with half the volume of chloroform and then counted; the amount of radioactivity contained in the aqueous layer was used for determining overall recovery and the amount of non-chloroform extractable material synthesized during the metabolism studies. In several experiments, 1 N NaOH was added to the tissue pellets resulting from the initial methanol treatment, and the samples were heated for 0.5 hr or more on a boiling water bath; the alkaline digest was neutralized and the radioactivity measured. This analysis of the residues was not performed routinely, since only a small portion (5–10 per cent) of the total initial radioactivity remained in this fraction; this percentage value did not vary appreciably with either substrate concentration or with incubation time.

The combined chloroform extracts were lyophilized in a rotating vacuum desiccator [19] (Speed Vac Concentrator model SVC, Savant Instruments, Hicksville, NY), the residues redissolved in 10 μl chloroform, and the tubes placed in an ice bath to prevent significant volume changes from occuring during the application of the samples to the t.l.c. sheets. The chromatograms were developed with hexane–acetone (4:3, v/v) in either a large, standard glass chromatography tank (for the 20 × 20 cm sheets) or in covered dishes normally used in the staining of microscope slides (for the 6 × 7 cm sheets); visualization of the cannabinoids was achieved by spraying the air-dried chromatograms with a 0.1% solution of Fast Blue B in 70% ethanol. The large (20 × 20 cm) t.l.c. sheets were used for determining changes in the metabolite distribution pattern with time. In addition to visualizing and recording the location of prominent cannabinoid spots on these larger t.l.c. sheets, the developed chromatograms were cut into strips (2 × 20 cm) for analysis with a radio-chromatogram scanner. After scanning, the chromatograms were reassembled by taping the strips to paper, and zones containing distinct spots were demarcated and aspirated directly into scintillation vials containing approximately 1 ml of 95% ethanol. Non-radioactive CBD, Δ^9-THC, 11-hydroxy-Δ^9-THC and 8α,11-dihydroxy-Δ^9-THC were used routinely as reference standards on the large t.l.c. sheets.

The small t.l.c. sheets (6 × 7 cm) were used in all other cannabinoid experiments; these chromatograms yielded a separation of the umetabolized substrate from its products, comparable to that achieved with the larger sheets, and could be developed in less than 10 min with the hexane–acetone solvent system. In some experiments, aliquots of non-radioactive Δ^9-THC or CBD were added prior to the chloroform extraction step to facilitate the visualization of the area containing the unmetabolized substrate; such additions were usually made only when very small amounts of unmetabol-

Table 1. Comparison of apparent kinetic constants for Δ^9-THC and CBD metabolism by rat and mouse liver*

Drug	Species	K_m (μM)+	V_{max} (nmoles/g protein/min
Δ^9-THC	Rat	16 ± 11	190 ± 40
	Mouse	13 ± 10	549 ± 174
CBD	Rat	16 ± 9	55 ± 17‡
	Mouse	6 ± 2	175 ± 49‡

* Data are based upon a comparison of Δ^9-THC and CBD metabolism by the same crude microsomal preparation obtained from six rat and seven mouse livers. Values are the means ± the standard deviations and are corrected for t.l.c. recovery.

+ None of the values is significantly different from any of the others by paired-*t* statistics ($P > 0.05$) [20].

‡ Significantly less than the corresponding rat or mouse Δ^9-THC value by paired-*t* statistics ($P < 0.05$) [20].

ized Δ^9-THC or CBD were anticipated. The t.l.c. areas containing the unmetabolized substrate and its metabolites were aspirated directly into scintillation vials containing 1 ml of 95% ethanol, as in the experiments with large t.l.c. sheets. All samples were counted in 10 ml Handifluor (Mallinckrodt, St. Louis, MO) or Aquasol (New England Nuclear Corp., Boston, MA). Counting was perfomed in a Nuclear–Chicago PDS/3-Isocap 300 liquid scintillation counter; the radioactivity values obtained were corrected for machine efficiency and quenching.

From the sum of radioactivity in the aqueous phase, in the chloroform extract spotted on the chromatogram, and in the tissue residue, the mean recovery value (± S.D.) was calculated to be 89% (± 11%). The recovery of the radioactivity applied to the t.l.c. sheets averaged 85% (± 10%). The overall recovery of the radioactivity originally added to the incubation vessels was approximately 76 per cent.

RESULTS

Kinetic aspects of Δ^9-THC and CBD metabolism in rat and mouse. The apparent K_m and V_{max} values presented in Table 1 were determined for CBD and Δ^9-THC in paired experiments using a crude microsomal preparation (20,000 *g* supernatant fraction) obtained from either mouse or rat liver; protein concentrations in the incubation mixture averaged 6 mg/ml for the rat and 3 mg/ml for the mouse experiments. After an incubation period of 15 min, labeled substrates and metabolites were extracted, concentrated to a final volume of 10 μl, and an aliquot of the concentrate was spotted on small chromatograms, which were developed and processed as described in Materials and Methods.

As may be seen in Table 1, there are no significant differences in the apparent K_m values for Δ^9-THC and CBD determined with either rat or mouse preparations. There are, however, significant species differences in the maximum rates at which Δ^9-THC and CBD are metabolized, as revealed by the apparent V_{max} values; the maximum rate of CBD metabolism in the mouse or in the rat is approximately one-third that of the corresponding rate of metabolism of Δ^9-THC. Furthermore, a comparison of the apparent V_{max} values in the two species indicates that the mouse 20,000 *g* supernatant fraction is much more active than the rat preparation for both cannabinoids.

Figure 1 is an example of an experiment to determine the linearity of Δ^9-THC and CBD metabolism with time when the substrate is not limiting. A rapid decrease in the rate of metabolism in the CBD samples is evident in both the mouse and rat preparations; in contrast, the Δ^9-THC rate slows markedly only after about 60 min. As in the Δ^9-THC portion of these experiments, the CBD concentrations used was substantially greater than the apparent K_m value (Table 1). Consequently, it is unlikely that the recorded cessation in CBD metabolism is due to a limited supply of substrate and, considering the Δ^9-THC results, cessation is not likely to be

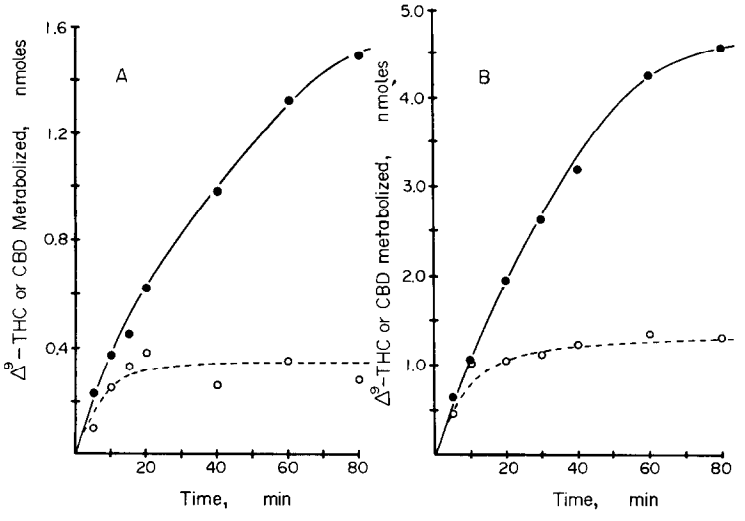

Fig. 1. Linearity of the rate of Δ^9-THC (●) and CBD (○) metabolism by crude hepatic microsome preparation. (A) Mouse preparation: protein concentration = 1.5 mg/ml; Δ^9-THC and CBD concentrations were 120 and 130 μM respectively. (B) Rat preparation: protein concentrations = 5 mg/ml in Δ^9-THC sample and 15 mg/ml in CBD sample; Δ^9-THC and CBD concentrations were 59 and 82 μM respectively.

attributable to a decreased viability of the mixed-function oxidase system. Enzyme inhibition by the CBD molecule itself is also an implausible explanation for the results, since, even with the high initial CBD concentration (80–130 μM), some metabolism, occurs. The apparent dependence of the inhibitory effect on a finite incubation time suggests that the effect is a consequence of the formation of CBD metabolites in sufficient concentration to inhibit the mixed-function oxidase system, and, consequently, CBD's own metabolism. Such inhibition might account for the observed apparent V_{max} differences between Δ^9-THC and CBD in both the rat and mouse (Table 1).

Time-dependent metabolite patterns. The characteristics of the time-dependent CBD and Δ^9-THC metabolite patterns can be seen in the bar graphs of the percentage distribution of radioactivity on the chromatograms (Fig. 2). In the solvent system used to develop the chromatograms, authentic 11-hydroxy-Δ^9-THC and 8α,11-dihydroxy-Δ^9-THC have R_f values of approximately 0.34 and 0.08 respectively.

Within the limits of the resolution of the t.l.c. system, the metabolism of CBD was judged to be qualitatively the same as that of Δ^9-THC in both the rat and the mouse; that is, there is a progressive increase in the polarity of both the CBD and Δ^9-THC products formed as a function of time. this increase in polarity is evidenced by a shift in the distribution of radioactivity to lower R_f values (Fig. 2). The increase in radioactivity remaining in the aqueous phase probably reflects the formation of the most polar metabolites since these products are not extractable into chloroform from the methanol-treated incubation medium. No detailed analysis of this aqueous phase was made, but in one experiment, [^{3}H]CBD was incubated for 2 hr under conditions similar to those used to obtain the data in Fig. 2; however, the pH of the incubation medium was varied prior to chloroform extraction. At pH 13, almost twice as much material remained in the methanol–water phase as at pH 2; therefore, at least some of the CBD metabolites remaining in the aqueous phase in the standard assay procedure appear to be acidic in nature.

Inhibition of metabolism by CBD. Although CBD has a demonstrable inhibitory effect on the hepatic mixed-function oxidase system both *in vivo* and *in vitro* [4–8], what is not clear is whether the compound responsible for this effect is unaltered CBD or a metabolite. The rapid decline in the rate of CBD metabolism in both rat and mouse preparations (Fig. 1) provides suggestive evidence that the inhibition of drug metabolism by CBD may actually be due to the formation and accumulation of an inhibitory product. As a test of this thesis, the *in vitro* effect of CBD metabolites on the demethylation of aminopyrine, as measured by the formation of [^{14}C]formaldehyde (HCHO), was examined indirectly and the results are presented in Fig. 3. Figure 3 is composed of three different experiments conducted simultaneously on three sets of samples, all of which contained the 20,000 *g* supernatant fraction derived from mouse liver plus the necessary cofactors and buffer solution. One set of samples, to which was added only a blank solution of ethanol and Pluronic in the same concentration used to suspend CBD, served as a control, while CBD was added to the other two sets

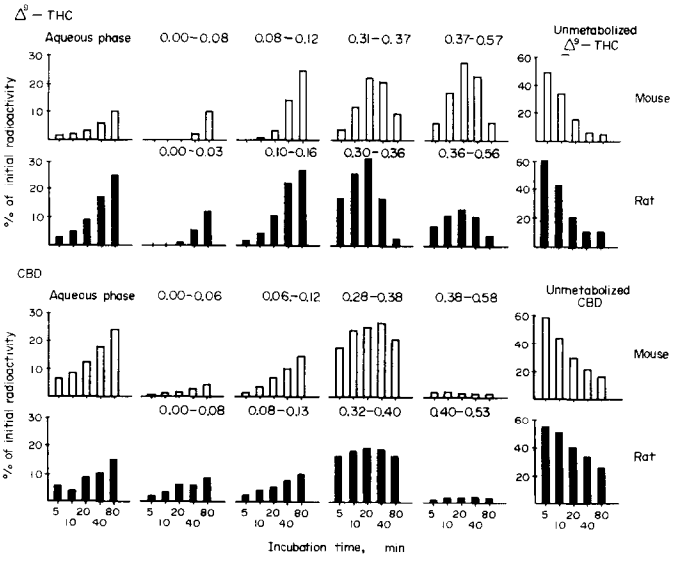

Fig. 2. Per cent distribution of initial radioactivity among selected t.l.c. zones. Mouse and rat 20,000 *g* supernatant fractions were incubated for varying periods of time and subsequently extracted and chromatographed on large t.l.c. sheets; the radioactivity in selected t.l.c. zones was measured and expressed as a percentage of the total radioactivity initially present in the incubation medium. Incubation volume = 250 μl. Cannabinoid and protein concentrations in mouse experiments were: CBD = 11 μM and 0.5 mg/ml; and Δ^9-THC = 6 μM and 3 mg/ml. Cannabinoid and protein concentrations in rat experiments were: CBD = 14 μM and 7.4 mg/ml; and Δ^9-THC = 16 μM and 3.2 mg/ml. The numbers above each bar graph are the R_f boundaries of the zones aspirated from the t.l.c. sheets. The aqueous phase bar graph represents the material not extractable by chloroform from the methanol-treated incubation medium. Not all of the areas on the t.l.c. are represented in the figure, and radioactivity values used to calculate the percent distribution were only corrected for t.l.c. recovery.

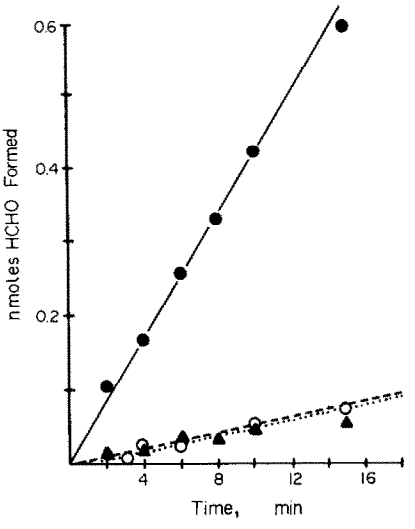

Fig. 3. Effects of CBD metabolites on aminopyrine *N*-demethylase activity in mouse hepatic 20,000 *g* supernatant fraction. Incubation conditions: protein concentration = 7 mg/ml; incubation volume = 50 μl; [^{14}C]aminopyrine and CBD concentrations were 90 and 10 μM respectively. All samples were initially incubated for 10 min in the absence of aminopyrine followed by a second incubation in the presence of aminopyrine for a period of time indicated on the abscissa. Control samples (●) not exposed to CBD at any time. T–1, CBD (▲) added before the first incubation. T–2, CBD (○) added after the first incubation.

(designated T-1 and T-2) but at different incubation times. CBD was added initially in the T-1 experiments, then the three sets of samples (control, T-1 and T-2) were incubated for 10 min at 37°, after which time they were all placed in an ice bath. CBD was added to the T-2 samples and all samples were then incubated at 37° for varying periods of time. If CBD metabolites are responsible for the inhibitory effects of CBD on the mixed-function oxidase system, two effects should occur in the experiments outlined above: First, in the CBD-preincubated samples (T-1), the amount of aminopyrine metabolized should be depressed, relative to control, throughout the entire period of the second incubation due to the presence of CBD metabolites formed during the initial incubation period. Secondly, in the T-2 samples to which CBD is added after the first incubation, inhibition of aminopyrine metabolism should also be evident, but the onset of inhibition delayed until sufficient CBD is metabolized.

In Fig. 3, the results show that prior incubation with CBD (T-1) did not influence the CBD inhibition of aminopyrine metabolism (T-2); the effects were the same in both sets of CBD-treated samples. These conclusions do not support the hypothesis that CBD metabolites are involved in the inhibitory effect; however, the results underscore the necessity for choosing the appropriate enzyme assay for such a study of drug metabolites.

Figure 3 illustrates that the inhibition of aminopyrine metabolism produced by prior incubation with CBD (T-1) did not influence the CBD inhibition of by CBD added subsequent to the first incubation period (T-2). the failure of the incubation time of CBD to affect differentially the metabolic rate of aminopyrine suggests that CBD itself is responsible for the observed inhibition, rather than its metabolites. This conclusion, however, was tempered by the results of subsequent experiments which compared the kinetics of aminopyrine and CBD metabolism *in vitro*. We observed that the amount of 20,000 *g* supernatant protein required to metabolize equivalent quantities of CBD and aminopyrine with the substrate concentrations used in Fig. 3 differed by one order of magnitude; the rate of CBD hydroxylation is much greater than is the rate of aminopyrine demethylation. Therefore, with the concentration of 20,000 *g* supernatant protein and CBD used to generate the data in Fig. 3, essentially all of the CBD would be metabolized in just a few minutes; and the effect of a progressive increase in inhibitory metabolite formation with time would be masked. Consequently, the experiment was repeated by measuring Δ^9-THC hydroxylation because the metabolic kinetic character-

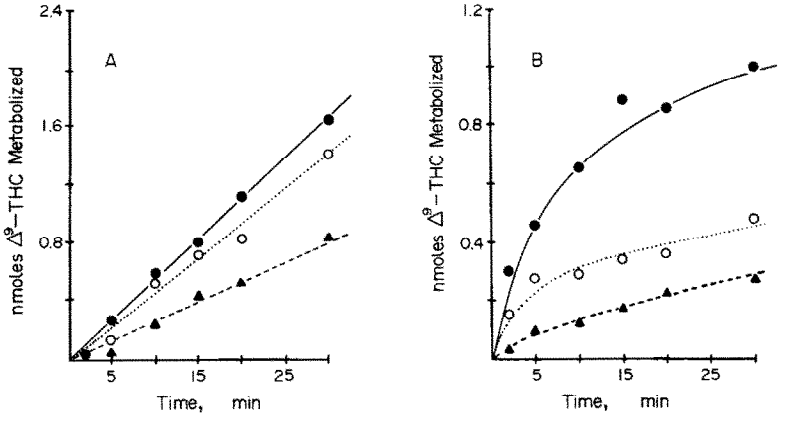

Fig. 4. Effects of CBD metabolites on [^{3}H]Δ^9-THC metabolism by mouse hepatic 20,000 *g* supernatant fraction. Incubation conditions: protein concentration = 3 mg/ml; incubation volume = 50 μl and CBD concentration = 10 μM. Experiments in A and B differ only in the Δ^9-THC concentration used: A = 155 μM, and B = 27 μM. All samples were initially incubated for 15 min in the absence of ^{9}-THC followed by a second incubation in the presence of ^{9}-THC for a period of time indicated on the abscissa. Symbols are identical to those used in Fig. 3.

istics of this reaction are similar to those of CBD hydroxylation. In Fig. 4A, it is evident that Δ^9-THC metabolism was depressed markedly in the preincubated, or T-1, samples, whereas the T-2 samples were depressed slightly and even this effect was only evident with the longer incubation times. When the Δ^9-THC concentration was reduced in order to decrease the extent of Δ^9-THC competition in the hydroxylation reaction, Δ^9-THC metabolism was sharply depressed in both treated groups (Fig. 4B). If CBD were the principal inhibitor, the data points representing T-1 samples would be reversed with those points representing T-2 in both 4A and 4B, because, with the protein and CBD concentrations used, over 50 per cent of the starting CBD would be metabolized during the first incubation period; therefore, the T-1 samples would be less inhibited than those in the T-2 group. Furthermore, in Fig. 4B, the curves representing the treated samples tend to parallel each other only after approximately 5 min; the time lag is interpreted as an indication that some metabolism of CBD must take place before the inhibition of Δ^9-THC metabolism can occur

DISCUSSION

The results of the comparative kinetic studies of the metabolism of Δ^9-THC and CBD in both rat- and mouse-microsomal systems indicate that the two drugs undergo biotransformation at significantly different rates. CBD is metabolized by the mixed-function oxidase systems from mouse and rat more slowly than is Δ^9-THC, as is evidenced by the apparent V_{max} values in Table 1. Additionally, the mouse preparation is approximately two or three times more active than that of the rat when either Δ^9-THC or CBD is the substrate. Despite these differences in V_{max}, the apparent K_m values determined for these two cannabinoids (Table 1) are not statistically different whether they are compared within or between species. Siemens and Kalant [21] reported apparent K_m and V_{max} values for Δ^9-THC of 135 μM and 570 nmoles/g of protein/min respectively; these values were obtained with a rat-liver 10,000 g supernatant fraction. Their apparent V_{max} and K_m values are much higher than the comparable values presented in Table 1; however, the apparent K_m of 16 μM for Δ^9-THC determined in the present investigation with rat-liver 20,000 g supernatant fraction is quite similar to the 28 and 15 μM values in the more purified liver microsomal preparations reported by Kupfer *et al.* [22] and Cohen *et al.* [23] respectively. The discrepancy between the Siemens and Kalant kinetic data and those found in Table 1 may lie in differences in the methods used for preparing the crude microsomal fractions or in differences in the method used to suspend the cannabinoids. The concentration of protein in their 10,000 g supernatant preparation was over three times greater than the protein concentration in the 20,000 g supernatant fraction used in the present study; furthermore, they added the cannabinoids as a suspension prepared with rat serum rather than with detergent. Nevertheless, these discrepancies in kinetic constants are not particularly disturbing in view of the crudeness of the enzyme preparations used in these types of studies. The relative differences in the rates of metabolism of Δ^9-THC and CBD and the species differences which have been noted (Table 1) are the important considerations; these undoubtedly reflect true differences, since the comparisons were made simultaneously in the same microsomal preparation.

The results of the biotransformation studies presented in Fig. 2 illustrate that the metabolite patterns of CBD and Δ^9-THC share common characteristics. As is demonstrated in this figure, both drugs are progressively metabolized to increasingly polar products, a phenomenon most clearly seen in the aqueous phase of Fig. 2, in which the cannabinoid content increases continuously with incubation time. The results also indicate that the separated metabolites are chromatographically very similar; that is, the R_f values for the metabolites of Δ^9-THC and CBD are practically identical in both rat and mouse. The most conspicuous difference in the pattern of Δ^9-THC and CBD metabolites in both species is the lack of primary metabolites of CBD found in the zone centered around an R_f value of approximately 0.47. Other differences may also exist but may not be apparent because of the limited resolution afforded by t.l.c. [12]. For example, each of the selected zones is probably composed of a mixture of CBD and Δ^9-THC metabolites which have similar R_f values but possess a hydroxyl group(s) in different positions on the basic molecule [12]. Similarities in the metabolism of Δ^9-THC and CBD, and the location of the hydroxyl groups on each of these molecules have been noted by others [24].

In addition to the comparative studies of biotransformation kinetics and of metabolite patterns of CBD and Δ^9-THC, an attempt was made to explain the marked decline with time in CBD metabolism which occurred in the presence of an excess concentration of this cannabinoid (Fig. 1). In both the mouse and rat, CBD metabolism follows a time course similar to that of Δ^9-THC, but unlike Δ^9-THC, CBD metabolism ceases abruptly after a 10- to 15-min incubation period. The reason for the cessation of metabolism is not clear; however, since the initial concentrations of CBD were several times the apparent K_m values (Table 1), and since some metabolism of CBD did occur (Fig. 1), inhibition of the reaction by unmetabolized CBD seems an improbable explanation. Subsequent experiments were designed to determine if the self-limiting CBD metabolism is dependent upon the production of an inhibitory metabolite.

Indirect evidence that the metabolites of CBD can inhibit the hepatic mixed-function oxidase system was obtained from the experiments to test the influence of CBD metabolism on aminopyrine *N*-demethylase and on Δ^9-THC hydroxylase activities (Figs. 3 and 4). In particular, the results of the Δ^9-THC hydroxylase experiments (Fig. 4) are consistent with the thesis that CBD metabolites, and not CBD itself, are responsible for the inhibition of the mixed-function oxidase system. Similar conclusions were drawn from a study of the pharmacokinetics of CBD in the liver [25]. These data demonstrated that the half-time for the prolongation of hexobarbital sleep time did not correlate with the very short half-time of CBD or its primary metabolite in the liver. The time course of other metabolites in the liver, however, can account for the duration of the CBD effect on drug metabolism *in vivo*, which, like the effect *in vitro*, may be a consequence of the formation of inhibitory metabolites.

Acknowledgements—The authors are indebted to Dr. Monique C. Braude, Division of Research, NIDA, for supplying the cannabis derivatives and for her advice and encouragement. The work was supported by USPHS Research Grant DA-00346.

REFERENCES

1. I. Izquierdo and M. Tannhauser, *J. Pharm. Pharmac.* **25**, 916 (1973).
2. R. Karler, W. Cely and S. A. Turkanis, *Life Sci.* **13**, 1527 (1973).
3. S. A. Turkanis and R. Karler, *Life Sci.* **17**, 569 (1975).
4. G. Jones and R. G. Pertwee, *Br. J. Pharmac.* **45**, 375 (1972).
5. W. D. M. Paton and R. G. Pertwee, *Br. J. Pharmac.* **44**, 250 (1972).
6. M. Fernandes, N. Warning, W. Christ and R. Hill, *Biochem. Pharmac.* **22**, 2981 (1973).
7. M. Fernandes, S. Kluwe and H. Coper, *Nauyne-Schmideberg's Archs. Pharmac.* **283**, 431 (1974).
8. A. J. Siemens, H. Kalant, J. M. Khanna, J. Marshman and G. Ho, *Biochem. Pharmac.* **23**, 477 (1974).
9. E. W. Gill, G. Jones and D. K. Lawrence, *Biochem. Pharmac.* **22**, 175 (1973).
10. R. Karler, W. Cely and S. A. Turkanis, *Res. Commun. Chem. Path. Pharmac.* **9**, 441 (1974).
11. R. Karler and S. A. Turkanis, in *The Therapeutic Potential of Marihuana* (Eds. S. Cohen and R. C. Stillman), p. 383. Plenum, New York (1976).
12. R. Mechoulam, N. K. McCallum and S. Burstein, *Chem. Rev.* **76**, 75 (1976).
13. I. M. Nilsson, S. Agurell, J. L. G. Nilsson, M. Widman and K. Leander, *J. Pharm. Pharmac.* **25**, 486 (1973).
14. B. Martin, S. Agurell, M. Nordqvist and J.-E. Lindgren, *J. Pharm. Pharmac.* **28**, 603 (1976).
15. B. Martin, M. Nordquist, S. Agurell, J.-E. Lindgren, K. Leander and M. Binder, *J. Pharm. Pharmac.* **28**, 275 (1976).
16. B. R. Martin, D. J. Harvey and W. D. M. Paton, *Drug Metab. Dispos.* **5**, 259 (1977).
17. O. H. Lowry, N. J. Rosebrough, A. L. Farr and R. J. Randall, *J. biol. Chem.* **193**, 265 (1951).
18. A. P. Poland and D. W. Nebert, *J. Pharm. exp. Ther.* **184**, 269 (1973).
19. R. W. Albers and O. H. Lowry, *Analyt. Chem.* **27**, 1829 (1955).
20. G. W. Snedecor and W. G. Cochran, in *Statistical Methods*, 6th Edn. Iowa State University Press, Ames (1967).
21. A. J. Siemens and H. Kalant, *Biochem. Pharmac.* **24**, 755 (1975).
22. D. Kupfer, I. Jansson and S. Orrenius, *Chem.-Biol. Interact.* **5**, 201 (1972).
23. G. M. Cohen, D. W. Peterson and G. J. Mannering, *Life Sci.* **10**, 1207 (1971).
24. S. Agurell, M. Binder, K. Fonseka, J.-E. Lindgren, K. Leander, B. Martin, I. M. Nilsson, M. Nordqvist, A. Ohlson and M. Widman, in *Marihuana: Chemistry, Biochemistry and Cellular Effects* (Eds. G. G. Nahas, W. D. M. Paton and J. E. Idänpään-Heikkila), p. 141. Springer, New York (1976).
25. R. Karler, P. Sangdee, S. A. Turkanis and H. K. Borys, *Biochem. Pharmac.* **28**, 777 (1979).